ABSTRACT

The analytical methods for calculating magnetic fluxes and losses in steel in one- and three-phase shunt reactors with the location of tie rods in the middle and outside the main leg of the magnetic system have been developed and presented in this article. For this purpose, finite element modelling was used, and nonlinear magnetic equivalent circuits were sub-stantiated. The results of the calculation of the main and stray losses in the magnetic system have been compared with their estimates obtained by the typical tests of the reactors.

KEYWORDS:

losses, magnetic flux density, numerical modelling, magnetic equivalent circuits, magnetic system, shunt reactor

Shunt reactor is designed to provide a significant inductance to ensure an economical and stable process of electric energy transmission "

The calculation of magnetic fluxes and losses in the magnetic system of high-voltage shunt reactors

1. Introduction

A shunt reactor (ShR) is a device with a winding wound on a core, i.e., the magnetic system (MS), or it can be without the magnetic core. It is designed to provide a significant inductance to ensure an economical and stable process of electric energy transmission [1,2]. In this work, we will consider high-voltage ShRs containing main legs with nonmagnetic gaps of two designs – with the arrangement of tie rods in the middle of the main legs and outside them.

Losses in the MC of the ShR can make up to 50 % of the total losses [1], and therefore, their calculation is an essential task at the operational design stage [2–6]. However, the issue is complicated because separating electrical steel losses and stray losses in parts of the ShR structure during measurements is practically impossible. The losses in the core and the stray losses are equal to the difference between total losses and ohmic losses [1].

The model of a single-phase ShR, which was developed using a three-dimensional CAD design software Pro/ENGINEER [6], is shown in Fig. 1. The main leg disks are made using radially laminated stack packets, the side legs and yokes are made using planar stacking of electrical steel (ES) sheets.

In the proposed analytical method, the magnetic flux density values used for the calculation of the losses in ES have been determined as in [2–6] through simplified steady-state models based on the magnet-ic resistances of a main leg with a winding of a single-phase reactor. At the same time, it has been assumed that the solenoid flux tubes of the magnetic field in the winding region are uniform over the entire height of the MS window. The protrusion of the magnetic flux in the gaps between the main leg disks is taken into account by an increase in their cross-section.

When calculating the losses in steel as in [2–6], the known dependences on the magnetic flux density of the specific losses component (remagnetization and eddy currents) on the thickness of the sheets of the corresponding ES brands have been used. As in [7], but with approximate constant coefficients, the increase of losses in the corner parts of the MC has been taken into account. That
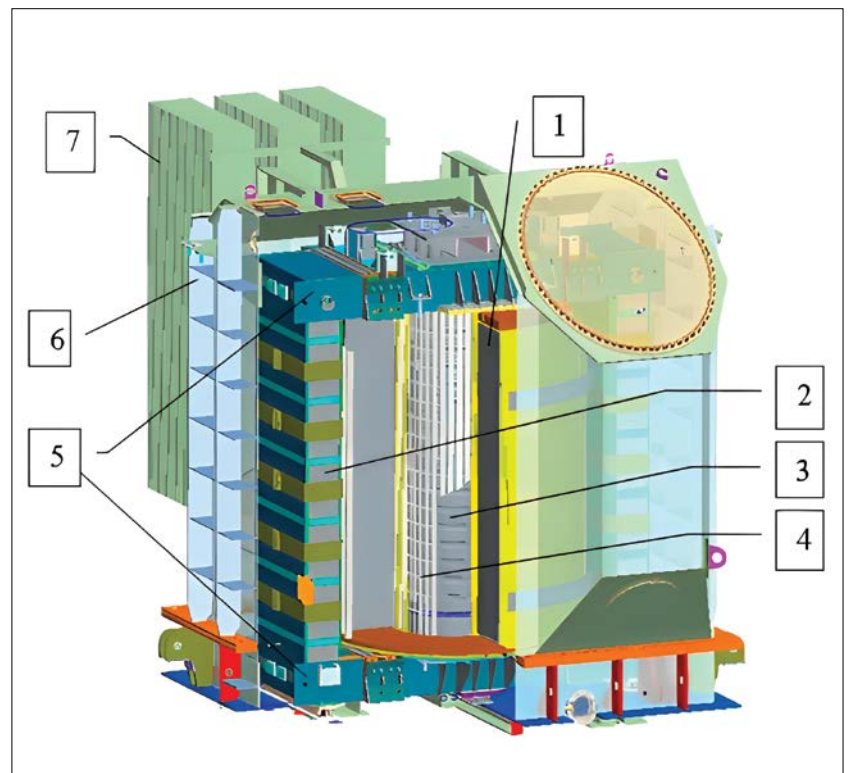
Figure 1. Model of a single-phase ShR: 1 – winding, 2 – MS from a main leg with gaps, side legs and yokes, 3 – main leg disks, 4 –electrostatic screen on the main leg, 5 –upper and lower core clamping plates, 6 – tank, 7 – external cooling system

Numerical modelling established that if there are holes in the yokes in the central stacks, additional eddy current losses occur

increase in the losses is due to the inhomogeneity of the magnetic field in the main leg disks, and it has been taken into account evenly with the same factor in the model.

The task becomes more complicated for three-phase ShRs – similarly to transformers [8], it is necessary to take into account the increase in losses due to the non-sinusoidal waveforms of the magnetic flux and significant specific losses for the fluxes that flow across the ES roll [9]. Numerical modelling established that if there are holes in the yokes in the central stacks, additional eddy current losses occur. They increase the overall losses in steel and can be identified by thermal imaging observations, which can also create local temperature hot spots.

Further improvement of loss calculation methods in the MS of the ShR remains an important task. For this purpose, for example, in [10], modelling by the method of finite elements in the transient analysis mode was applied, but of single-phase ShR. At the same time, a discrepancy of 26 % between the analytical and numerical calculation of the losses in steel has

been indicated. The same method was used in [11] to study the three-phase ShR with an MS without side legs.

It should be noted that analytical methods are necessary and computationally efficient tools for multivariable optimization calculations of ShR. For this, magnetic equivalent circuits (MEC) can be applied. For the MEC model development, it is advisable to draw the experience [6] of numerical modelling by finite element analysis (FEA) methods.

This article aims to present the development of a methodology for the analytical calculation of magnetic fluxes using nonlinear MEC, as well as the basics of the stray losses calculation in the magnetic systems of shunt reactors containing main legs with nonmagnetic gaps.

2. The design of the shunt reactor with gaps in the core of the magnetic system

Geometry under consideration has winding, main and side legs, legs with

yokes between them, and there are non-magnetic gaps in the magnetic circuit. A simplified sketch of the MS in the case of a single-phase ShR is shown in Fig. 2a. It has been assumed that the main leg of the MS consists of two radially stacked outer disks and N internal disks of the same height h_k and h, with the same internal d and external D diameters. There are gaps of size δ_k between the yokes and the outer disks and gaps of size δ between the inner disks. The winding has an average diameter, radial size, and height of D_0, a_0, H_0.

In Fig. 2(a), the following quantities are marked: b_k - the width of the channel that spreads from the main leg to the winding, Δ_0 - the height of the winding above the last internal gap in terms of main leg height, MO_1 – the interaxial distance between the main and side leg, H_{0k} – the height of the MS window, B_P – the width of yoke stacking. Three-phase designs can contain side legs or be without them. Tie rods can be placed in the middle or outside of the MS main legs. In the first case, vertical holes are created in the yokes by utilizing a special stacking method for the
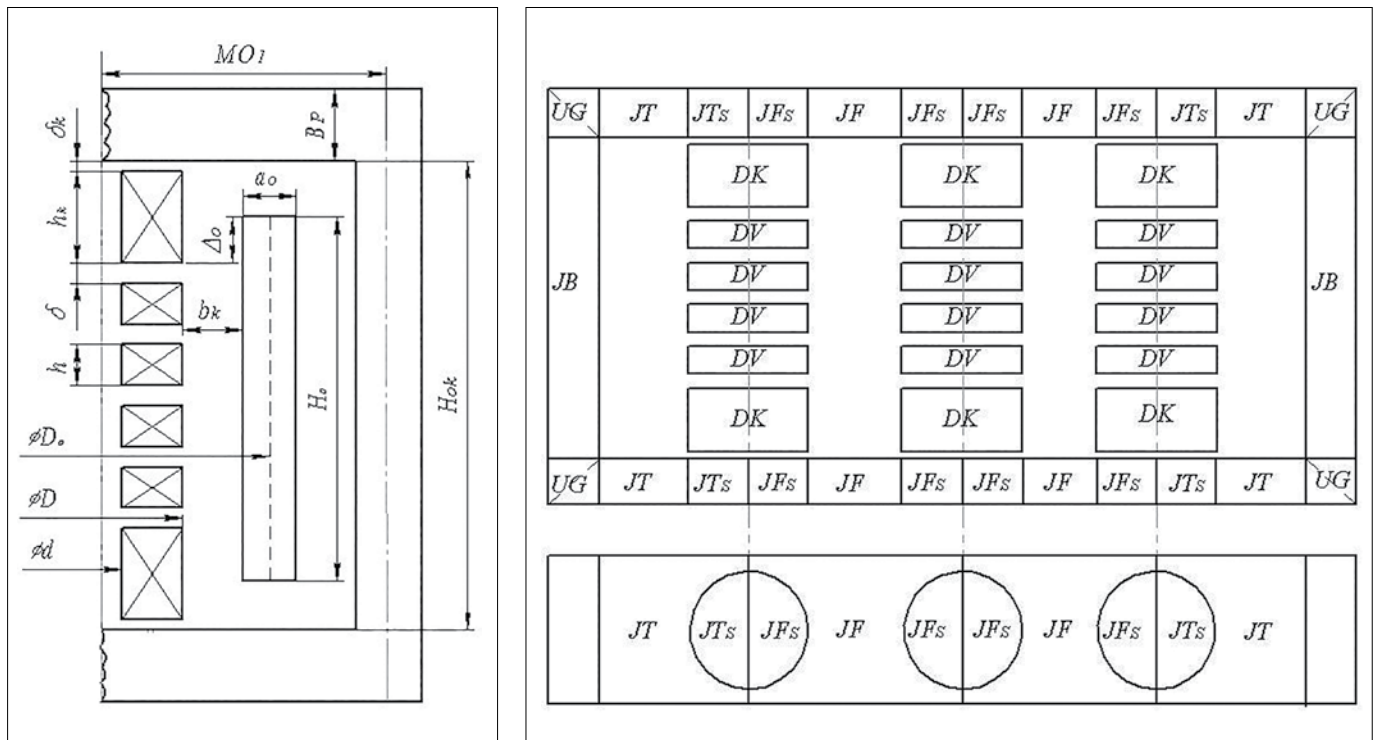
Figure 2. The design of ShR with gaps in the MS main leg: (a) a calculated model of the main leg with a winding, (b) a sketch of an MS with side legs of a three-phase reactor

sheets that allows the placement of the main leg tie rods.

Fig. 2(b) shows a sketch of the most developed MS with side legs of a three-phase reactor with a conditional breakdown into parts with characteristic features of the distribution of magnetic fluxes and losses. On the cross-section of the central yoke stacking, the following are marked: DV – internal disks, DK – outer disks, JB – side leg, JT –yoke, JF – interphase yoke, UG – yoke corners, JTs – end yoke-main leg, JFs – interphase yoke-main leg.

3. The calculation of the fluxes in the magnetic systems of reactors using magnetic equivalent circuits with concentrated parameters

3.1. Basic assumptions in the development of magnetic backup circuits

a) The magnitude of the magnetic flux in the main leg and in the winding channels does not depend on the yoke and side leg resistance, which is justified in the case of unsaturated yokes at the reactor's operating conditions.
b) The magnetic flux in the main leg is distributed evenly along the height of the winding and at the ends of the winding. The flux from the channel winding can flow into the outer disk and the yoke.
c) The magnetic flux in the yoke stackings is distributed in proportion to the cross-sectional area of the main leg and the winding channel over the thickness of the stack. The flux from the winding channel, which is outside the thickness of the yoke, can flow in the end region of the stacking of the yoke. There is no flux flowing between adjacent stackings (sub-stackings).
d) In the yoke stackings of three-phase MSs with side legs, the fluxes are redistributed by taking into account the different magnetic resistances of the individual sections of the branches (except for the central stacking with holes for the rod).
e) In the central stacking, only a part of the flux between the adjacent main legs can flow into the gap with holes for the rods. The rest of the flux enters normally to the plane of the long sheets

between the main legs of the adjacent phases.
f) To a large extent, assumption a) is ensured by the fact that the nominal value of the magnetic flux density in the MS main leg is selected in such a way as to ensure the magnetic operating point is in the linear region of the current-voltage characteristic of the reactor, not only in the operating modes but also at fairly significant multiples of that can occur in the fault conditions, such as short circuit current [1].

Assumptions b) – e) are formulated in this work based on the studies of the numerical models of reactors using FEA methods.

Assumption a) on the independence of the magnetic flux in the main leg from

the distribution of the fluxes in the yokes in the absence of their saturation allows sequentially considering the MEC of the main leg with the winding (primary circuit) and the stacked MECs (secondary circuits) of the MS reactor yokes and side legs. The interaction of the specified MECs is based on the linear superposition of the magnetic fluxes in the MS of the reactor, which generates the operating current in the winding, which can be used in this case.

3.2. Magnetic equivalent circuits of the main leg with the reactor winding

MEC is used for the calculation of the magnetic fluxes in the region of the MS core and the winding, which is shown in Fig. 3. The following are marked: linear
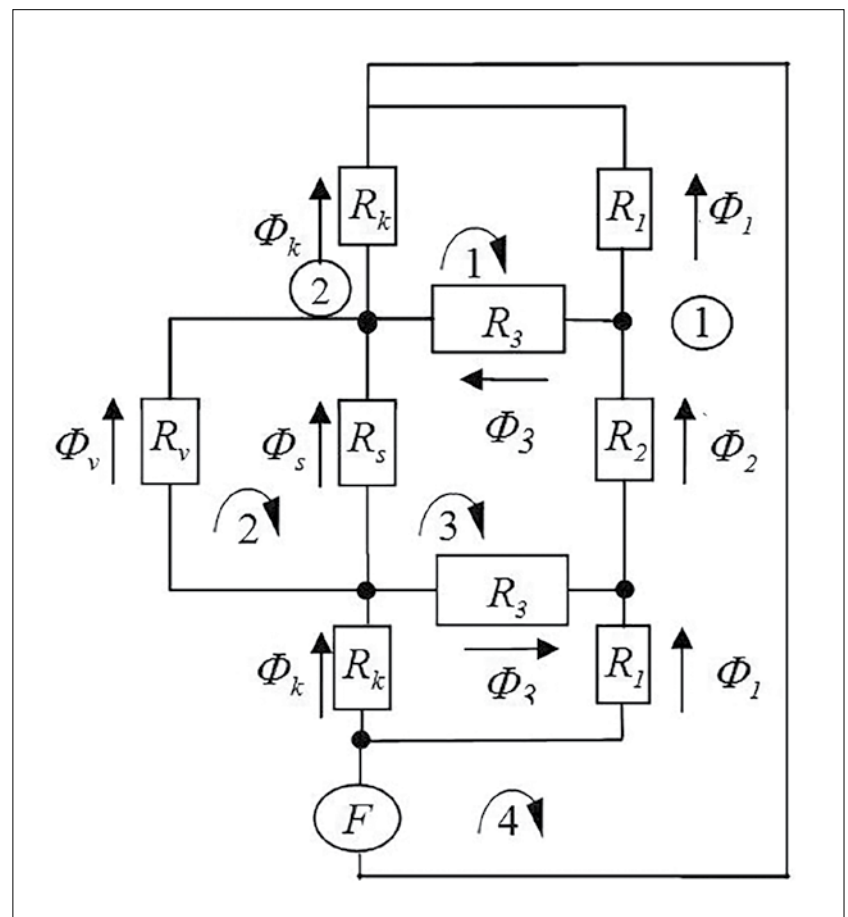
Figure 3. MEC of the main leg with the reactor winding

> ## Geometry under consideration has winding, main and side legs with yokes between them, and there are nonmagnetic gaps in the magnetic circuit

Magnetic equivalent circuits were used for the calculation of the magnetic fluxes in the region of the MS core and the winding

magnetic resistances of the parts between channels' end of the winding and yoke is R_1, between winding and main leg R_2, and between end of the winding to the end disk is R_3, the channel inside the main leg has magnetic resistance R_v, as well as the nonlinear magnetic resistances R_s of the internal disks steel and the gaps between them, and the resistance of steel R_k of the outer disk that also takes into account the space between it and the yoke.

To determine the parameters of the magnetic resistances of the MEC of the main leg, we will consider the results of the numerical studies of magnetic fluxes in the area of the winding and the main leg of the MS of a single-phase ShR. Taking into account symmetry, one-eighth of the complete geometry can be used for the analysis [6] – Fig. 4(a). Fig. 4(b) shows the spatial grid of the numerical model.

Fig. 4(c) presents the results of a numerical study of the distribution of the total magnetic flux density in the upper part of

the MS main leg at the yoke and side leg of 110 MVAr single-phase reactors. It is noticeable that the inner disks of the main leg are loaded evenly, and the outer ones more intensively. Note that the magnetic flux density value is not the same across the width of the yokes (by the stacks). The loading of the radial cross-section of the main leg disks by the magnetic flux is also uneven. The magnetic flux from the ends of the winding locally loads the parts of the yokes adjacent to the winding and then the side legs.

Fig. 5(a) shows the distribution of the axial magnetic flux density of the magnetic field at the end of the winding. The axial component of the field in the winding-yoke channel is maximal at the inner generating winding and decreases linearly towards the outer generating winding. Also, the axial field decreases linearly (almost to zero) towards the surface of the outer disk.

The distribution of the radial component of magnetic flux density in the upper part

of the main leg is shown in Fig. 5(b). The radial flux that flows from the winding to the outer disk is closed in the channel, which is located in the area where the end of the winding exceeds the last internal gap between the disks. It has also been determined that the flow of the magnetic flux outside the winding can be neglected due to its insignificant values, as well as due to its closing in the MS window through the yokes or outside the window (transverse axis of symmetry of the reactor), through transverse magnetic shunts to the surface of the yokes.

The provided observations and the assumptions of the methods [3, 4] allow us to determine the parameters of magnetic resistances of the MEC in Fig. 3.

The magnetic linear resistance between the ends of the winding and the yoke is calculated according to the ratio of the gap between the end of the winding and the yoke of the magnetic conductor to the area of the channel, limited by a third of the radial size of the winding and the main leg-winding channel, as measured from the inner forming winding

$$R_1 = (Hok - Ho)/2\left[\mu_0\pi\left((D_O - a_O/3)^2 - (D_O - a_O - 2/3\,b_K)^2\right)/4\right]^{-1}.$$

In order to develop an accurate magnetic equivalent circuit model of the reactor, finite element method calculation and analyses were used
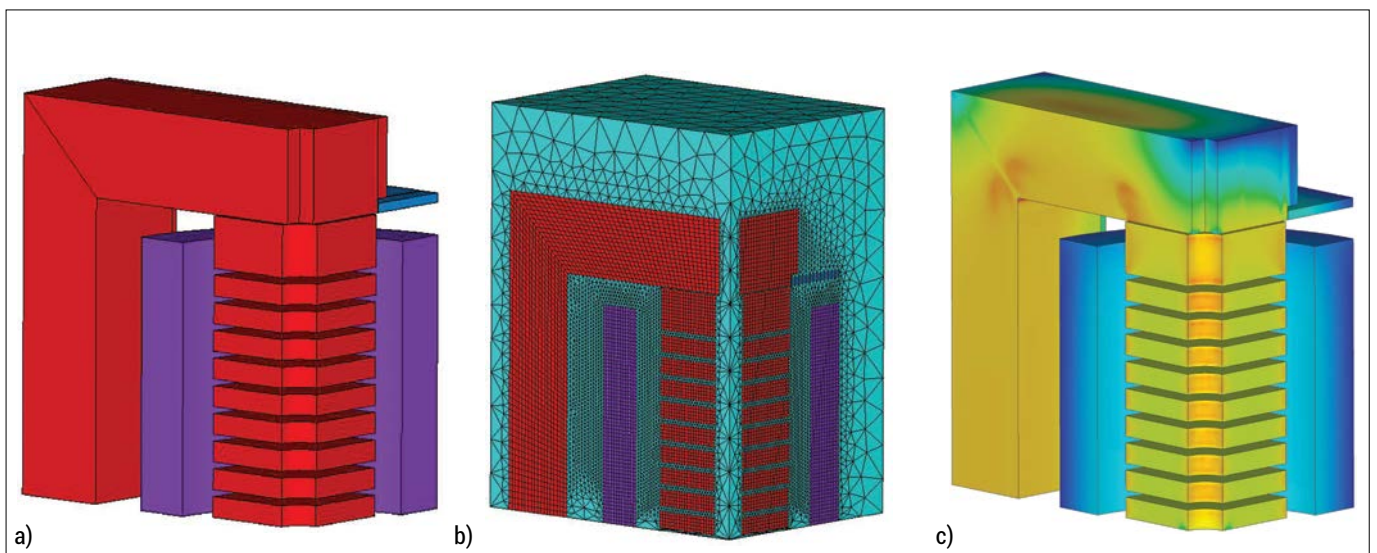
Figure 4. Finite element modelling of magnetic fluxes in the winding and core region of a single-phase ShR: (a) geometry of the calculation model, (b) finite element mesh, (c) the distribution of magnetic flux density in the main and side legs, yokes

An improved methodology of the stacked magnetic equivalent circuits was used for the yoke and side leg of the single-phase reactor

The magnetic resistance of the main leg-winding channel is determined by the height of the winding by the coupling of the turns of the winding within a third of the radial size of the winding from the inner surface of the winding, minus the section of the main leg with the correction for the expansion of the gaps [3, 4]

$$R_2 = Ho\left[\mu_0\pi\left((D_O - a_O/3)^2 - (D + 1.5\varepsilon)^2\right)/4\right]^{-1}$$

The magnetic resistance of the channel between the end of the winding and the outer disk is calculated from the gap between the outer surface of the main leg and the inner surface of the winding, referred to as the area of the channel "winding-outer disk", in which the end of the winding is above the last internal gap

$$R_3 = b_K\left[\mu_0\pi(D_O - a_O)\Delta_o\right]^{-1}.$$

The magnetic resistance of the channel inside the main leg is also calculated with the correction for the expansion of the gaps .

$$Rv = Hok\left[\mu_0\,\pi(d - 1.5\varepsilon)^2/4\right]^{-1}.$$

Magnetic nonlinear resistances in the inner and outer parts of the main leg are calculated as a series connection of the nonlinear resistances of the steel disks of the main leg, taking into account the

dependence on the magnetic flux density by the permeability of the electrical steel $\mu'(B)$ and the linear resistances of the corresponding gaps

$$R_s = \frac{h}{\mu_0\mu'(B)S_a}(n_z - 1) + \frac{\delta}{\mu_0 S_\varepsilon}n_z,$$

$$R_k = \frac{h_k}{\mu_0\mu'(B)S_a} + \frac{\delta_k}{\mu_0 S_k},$$

where S_v are the active sections of the inner ($v = z$) and outer ($v = k$) disks of the main leg, and n_z is the number of internal gaps of the main leg. When calculating the magnetic resistance of the gaps between the disks, the protrusion of the magnetic flux (Fig. 5b) is taken into account with a conditional expansion of the width of the disk by the amount $\varepsilon = \beta/\pi ln(1 + h/\beta)$ [3, 4]. At the same time, it is accepted that $\beta = \delta$ for internal gaps and $\beta = 2\delta_k$ for extreme gaps. The equivalent cross-sectional areas are defined as $S_v = \pi/4\left[(D + 2\varepsilon)^2 - (d - 2\varepsilon)^2\right]$.

The system of Kirchhoff equations for determining the fluxes in a main leg with a winding according to the MEC

$$\Phi_1 R_1 - \Phi_3 R_3 - \Phi_k R_k = 0, \quad \Phi_v R_v - \Phi_s R_s = 0,$$
$$\Phi_2 R_2 + 2\Phi_3 R_3 - \Phi_s R_s = 0,$$
$$\Phi_s R_s + 2\Phi_k R_k = I_n \sin(\omega t),\; \Phi_1 - \Phi_2 + \Phi_3 = 0,$$
$$\Phi_3 + \Phi_v + \Phi_s - \Phi_k = 0, \tag{1}$$

where $\omega = 2\pi f$ at industrial frequency f = 50 or 60 Hz.

The system (1) is nonlinear in the resistances R_s and R_k, depend on the corresponding fluxes Φ_s and Φ_k. The solution of the system of equations is determined for a given set of points in time t = 0, Δt..1/f with a step of Δt. In the first step, a magnetic flux of the order of 0.1 Wb is taken as the initial value. Next, the solution of the linear system of equations with respect to the fluxes is determined. Then, the magnetic permeability of steel is successively refined according to the value of the calculated induction. The values obtained in the previous step are taken as initial values in the next time step.

Thus, the MEC of a main leg with a winding (Fig. 3) and the presented algorithm provide a determination of the magnetic fluxes and losses in the inner DV and in the outer DK disks of the main leg, as well as the determination of the fluxes of the main leg with a winding, which are closed to the system of the yokes and side legs.

3.3. Stacked magnetic equivalent circuits of the yoke and side leg of the single-phase reactor

In single-phase MS, the magnetic flux Φ_k of the outer disk of the MS main leg and
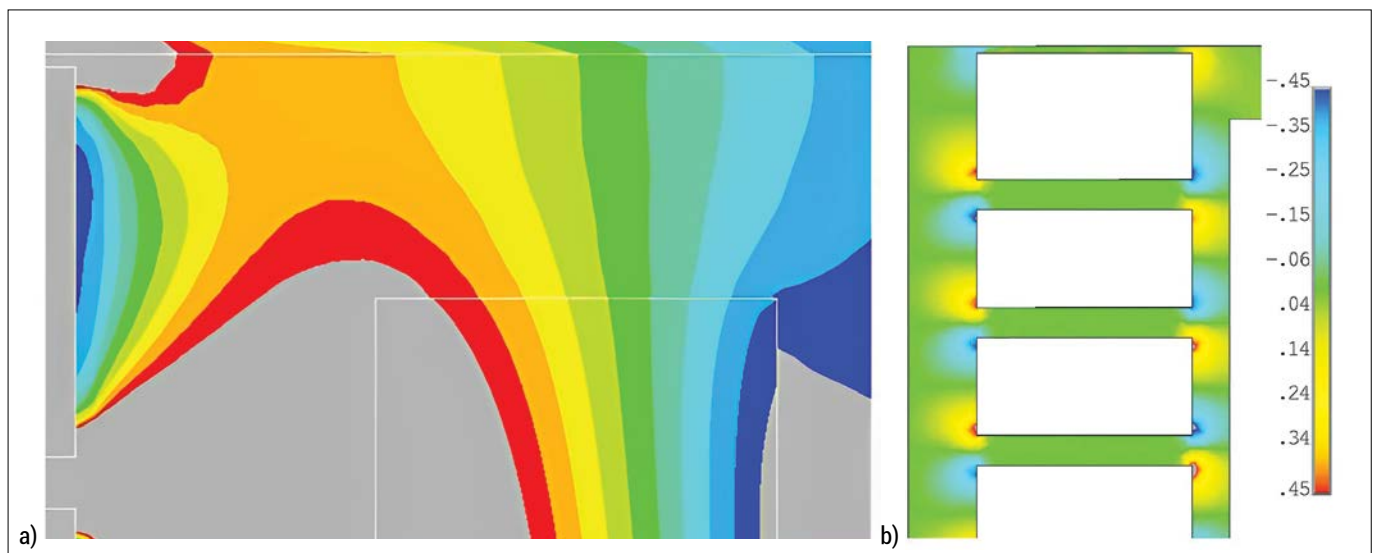
Figure 5.Distribution of magnetic field induction: (a) axial component at the end of the winding, (b) radial component in the adjacent zones of the upper end and inner disks of the main leg

The development of an appropriate equivalent circuit by introducing magnetic resistance normal to the planes of the specified stacks is a difficult task due to the complex geometry in three dimensions of the yoke structure
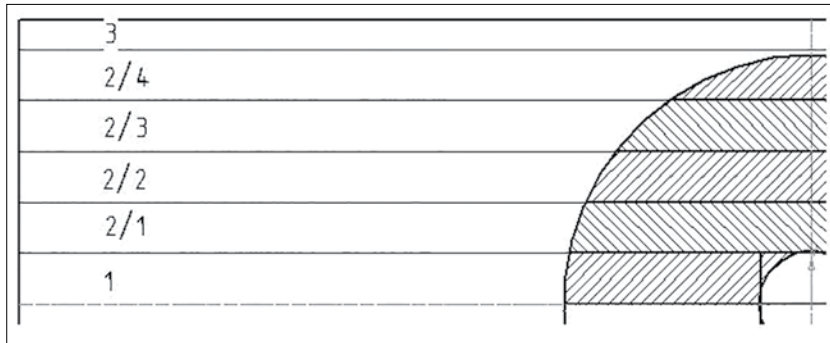
Figure 6. Projection of the yoke stacks on the cross-section of the main legs with the hole
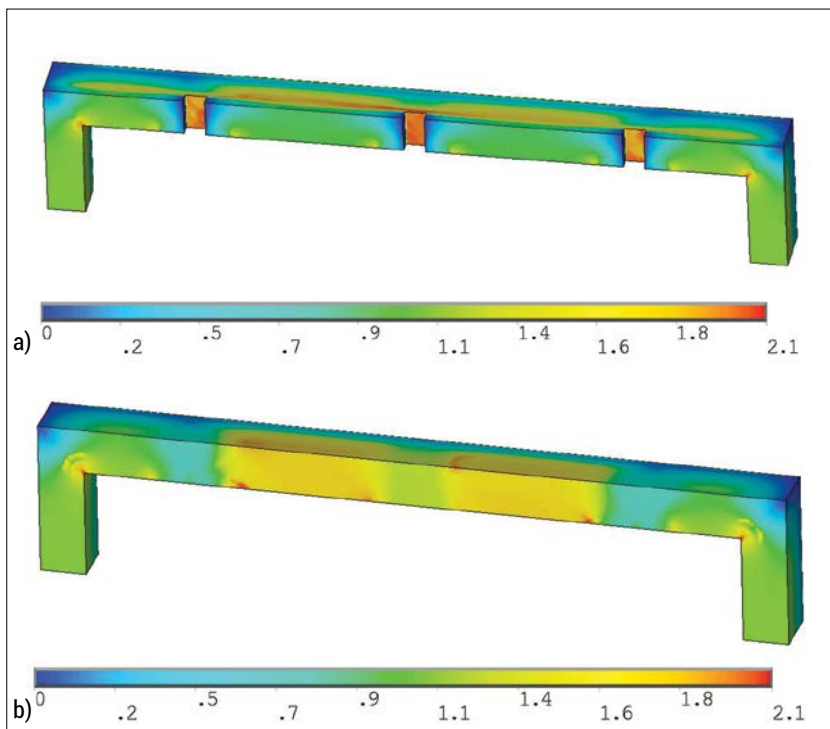
Figure 7. Distribution of the magnetic flux density component, which is directed along the steel rolling in the yokes of MS three-phase reactors with a 120 MVAr capacity: (a) design with holes for the main leg tie rods, (b) without holes

The magnitudes of the magnetic flux density in the interphase part of the yokes are determined by the fluxes in the MS main legs, similarly as in the case of the three-leg MS of transformers

the flux Φ_1 from the end of the winding according to the circuit of Fig. 3 are closed in stacks of yokes and side legs proportionally to the cross-sectional area of the main leg across the width of the stack (shaded in Fig. 6).

Since the stacks of the MS yoke have a significant thickness, they must be divided into substacks for a more accurate calculation of the flux distribution in these parts of the yoke; for example, stack 2 in Fig. 6 is divided into substacks 2/1, ..., 2/4. A stack with the number 1 is highlighted separately, with its width corresponding to the size of the hole for the tie rod.

Thus, the fluxes in the i-th stack of the yoke, taking into account the accepted assumption c), are calculated according to the formula ,

$$\Phi^i = \begin{cases} \Phi_k S_k^i/S_k + \Phi_1 S_1^i/S_1, & at \quad i = 1..N-1 \\ \Phi_k S_k^i/S_k + \Phi_1\left(S_1^i + S_1^0\right)/S_1 & at \quad i = \mathrm{N} \end{cases}'$$

where N is the number of substacks of the yoke, S_k^i, S_1^i is the cross-sectional area of the main leg and the channel above the winding along the i-th stack (shaded in Fig. 6), and S_1^0 is the channel above the winding, which is outside the yoke.

3.4. Stacked yoke magnetic equivalent circuits of the three-phase reactor with side legs

Fig. 7 shows the results of numerical research of the distribution of the component of magnetic field induction, which is directed along the steel rolling in the yokes of MS three-phase reactors with a 120 MVAr capacity: (a) design with holes for the main leg tie rods, (b) without holes.

If there are holes for the rod, only a part of the flux between the adjacent main legs is closed through the sheets of the interphase part of the yoke (central stack 1 in Fig. 6). The remaining part of the flux flows into the long sheets of the neighbouring 2/1 stack, almost doubling the magnetic flux density in them.

The development of an appropriate equivalent circuit by introducing magnetic resistance normal to the planes of the specified stacks is a difficult task due to the complex geometry in three dimensions of the yoke structure in the studied location.

To solve this issue, magnetic fluxes wave-

forms, which are excited by the adjacent phases' main legs and closed in the indicated stacks, were analyzed. For example, Fig. 8 shows the results of numerical studies of the three-dimensional model of the 120 MVAr reactor. The fluxes of two adjacent phases are marked as Φ_A^1 and Φ_B^1. The flux passing along the sheets between the phases alongside the steel sheets is denoted as $\Phi_{AB}^{\parallel}$, and the flux that exits normally to the sheets is denoted as $\Phi^{\perp}$. It was established that the following relations are valid between the specified fluxes

$$\Phi_{AB}^{\perp} = \left(\Phi_B^1 + \Phi_A^1\right)/2, \quad \Phi_{BC}^{\perp} = \left(\Phi_C^1 + \Phi_B^1\right)/2,$$

$$\Phi_{AB}^{\parallel} = \left(\Phi_B^1 - \Phi_A^1\right)/2, \quad \Phi_{BC}^{\parallel} = \left(\Phi_C^1 - \Phi_B^1\right)/2.$$

In the absence of a hole for the tie rod, the nature of the magnetic flux circuit (Fig. 7b) makes it possible to use the MEC of the MS stacks, which is shown in Fig. 9. The nonlinear supports of the *i*-th stack of the end and interphase part of yoke, side leg are marked

$$R_{jt}^i(B) = MO_1\left[\mu_0\mu'(B)S_{jt}^i\right]^{-1},$$

$$R_{jf}^i(B) = MO/2\left[\mu_0\mu'(B)S_{jf}^i\right]^{-1},$$

$$R_{jb}^i(B) = \left(H_{ok} + B_{Pi}\right)\left[\mu_0\mu'(B)S_{jb}^i\right]^{-1},$$

where $S_{jt}^i, S_{jf}^i, S_{jb}^i$ are the cross-sectional areas of the i-th stack of the end and interphase part of the yoke, side leg, BP_i is the width of the i-th stack of the yoke.

In the stacks without the rod holes of three-phase MSs with side legs, the values of the fluxes are determined according to the substitution circuit (Fig. 9) at the given main leg and winding fluxes ($\Phi_A^k, \Phi_B^k, \Phi_C^k$, k=2..N) and the given fluxes from the sheets of the central stack ($\Phi_{AB}^{\perp k}, \Phi_{BC}^{\perp k}$), where N is the total number of stacks and substacks of the yoke. $R_{jt}^k, R_{jf}^k, R_{jb}^k$ are supports of *k* stacks of the end and interphase parts of the yoke, side leg.

The system of Kirchhoff equations for determining the fluxes in yoke stacks according to the model (Fig. 9) is compiled for nodes 1–5 and circuit 1

$$\Phi_{j5}^i - \Phi_{j1}^i = \Phi_A^i, \quad \Phi_{j1}^i - \Phi_{j2}^i = \Phi_{AB}^{\perp i}, \quad \Phi_{j2}^i - \Phi_{j3}^i = \Phi_B^i,$$

$$\Phi_{j3}^i - \Phi_{j4}^i = \Phi_{BC}^{\perp i}, \quad \Phi_{j4}^i - \Phi_{j5}^i = \Phi_O^i,$$

$$2\Phi_{j1}^i R_{jf}^i\left(B_{j1}^i\right) + 2\Phi_{j2}^i R_{jf}^i\left(B_{j2}^i\right) + 2\Phi_{j3}^i R_{jf}^i\left(B_{j3}^i\right) + 2\Phi_{j4}^i R_{jf}^i\left(B_{j4}^i\right) +$$

$$+ \Phi_{j5}^i\left(2R_{jt}^i\left(B_{j5}^i\right) + R_{jb}^i\left(B_{j5}^i\right)\right) + \Phi_{j6}^i\left(2R_{jt}^i\left(B_{j6}^i\right) + R_{jb}^i\left(B_{j6}^i\right)\right) = 0. \tag{2}$$
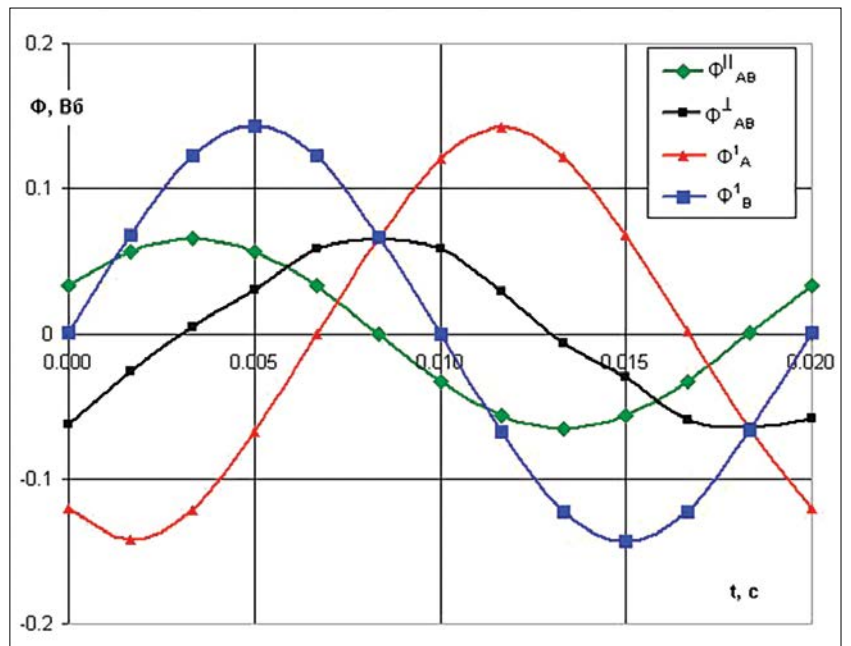
Figure 8. The change in time of the magnetic fluxes that are excited by the main legs of the adjacent phases and that are closed in the central stacks of the yoke
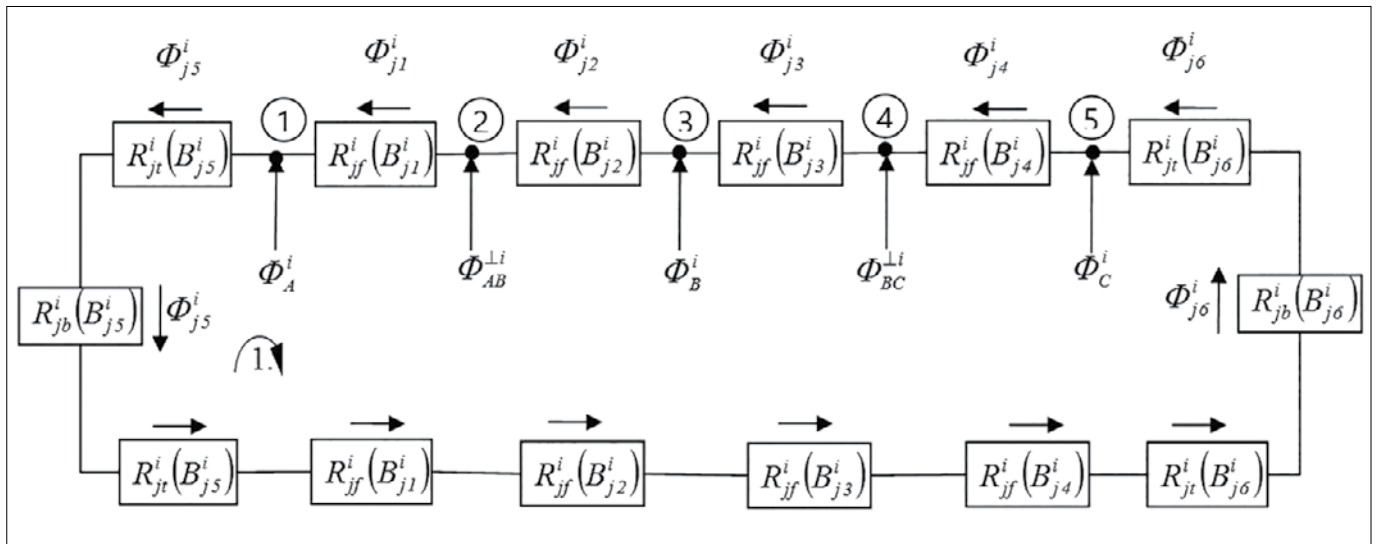
Figure 9. MEC of MS stacks with side legs

The stacked calculation of the magnetic fluxes in the yokes determines the distribution of flux density B_j and the corresponding specific losses $p(B_j^i)$ in each stack

The system of equations is nonlinear, and its solution is determined similarly to system (2), step by step, in time intervals. Due to the symmetry of the load and the design of the MS, the highest magnetic flux density values for the period occur in parts j1 and j4, j2 and j3, j5 and j6, and are mutually equal, as shown in Fig. 9.

If there is no gap under the tie rod in the central stack, the values of the normal fluxes, according to expressions in (8), take zero values. In this case, the calculation (5) is performed for all yoke stacks, including the central.

3.5. Stacked yoke magnetic equivalent circuits of the three-phase reactors without side legs

The magnitudes of the magnetic flux density in the interphase part of the yokes are determined by the fluxes in the MS main legs, similarly as in the case of the three-leg MS of transformers [7]. The non-uniformity of the flux in stacks, caused by the non-uniform loading of the flux from the main leg, is taken into account according to the circuit of Fig. 6.

If there are holes for the rods in the central stack, the amount of flux passing along and normal to the sheets is calculated according to the relation (4). In the yokes, the flux that enters from the main leg and the winding channel across the steel sheets returns and goes into the interphase part of the yoke. At the same time, a part of the flux leaks at the end of the yoke. Numerical research has established that the leakage is about 25 %.

4. The calculation of losses in the magnetic systems of shunt reactors

4.1. Losses in the corner parts of charging with a yoke

In the parts of the MS yoke, as in transformers [7], the magnetic flux turns, and accordingly, the movement is not in the direction of the steel rolling. During the transitions of the magnetic fluxes through the gaps at the junction of the ES sheets, currents occur normally to the sheets, as a result of which eddy currents arise in the planes of the sheets. In particular, for an oblique joint, the losses depend on the grade of steel, the amplitude magnetic flux density B in the corner, the width of the sheets b, and half of the length of the overlap of the sheets lk, which is determined along the axis of the sheets. The specified factors are taken into account by known empirical coefficients of loss increase [7] $k_{UG} = k_{pk}^\gamma (B,b,lk)$.

4.2. The irregularity of the flux in the yokes

The stacked calculation of the magnetic fluxes in the yokes determines the distribution of flux density B_j and the corresponding specific losses $p(B_j^i)$ in each stack. In addition, the non-sinusoidal factor (16) is calculated in each stack. The average flux density in the cross-section of the yoke and the averaged losses are determined by the expressions

$$B_j^s = 1/S_j \sum_{i=1}^N B_j^i S_j^i, \quad P_j^s = 1/S_j \sum_{i=1}^N p\left(B_j^i\right) \cdot k_{нc}^i \cdot S_j^i.$$

The loss increase factor depends on the ratio $k_j = P_j^s / p(B_j^s)$. For the end and interphase part of the yoke, side leg, the averaged flux density B_{jt}, B_{jf}, B_{jb} and and the coefficients k_{jt}, k_{jf}, k_{jb} and are determined accordingly.

4.3. Losses in the main leg disks

From the calculation of the distribution of the magnetic fluxes in the main leg according to the circuit from Fig. 3, the average value of the flux density B_s in the volume of the main leg is determined. Due to the gaps between the disks and the protrusion of the field (Fig. 6(b)), the magnetic flux density is unevenly distributed, increasing towards the edges of the disk, thus increasing the losses determined by the average value due to the nonlinear dependence of the losses on flux density.

For example, Fig. 10(a) shows the intensity of magnetic flux density in the lower half of the main leg disk. The minimum value in Fig. 10(b) is determined from the ratio of the geometric cross-section of the main leg S_T to the equivalent area S_ε as $B_{min} = B_s S_T / S_\varepsilon$.

To study the saturation of the disk, a local MEC was developed, in which the cylindrical volume of the lower half of the disk is divided into ring elements responsible for the conductivity in the vertical and horizontal directions, with different nonlinear characteristics of the ES in the longitudinal and transverse directions of the rolling [9]. A uniformly distributed flux from the inner gap is added to the lower nodes of the grid, and a flux from the protrusion zone is added to the side nodes, which uniformly decreases to zero in the middle of the disk height. The results of applying the circuit for the disk of the 110 MVAr reactor are shown in Fig. 10(c) in the form of flux density distribution at the lower edge of the disk (B_{KP}) and along the middle of the disk height B_{CEP}.

The calculation studies of the proposed equivalent circuit determined that with a nominal average flux density in the main legs of 1.2–1.5 T, while the intensity of the highest flux density at the edge of the disk reaches 1.8 T. At the same time, the zone of increased flux density (Fig. 10(b)) is determined by the amount of protrusion and is equal to $t = \varepsilon(B_{max}/B_{min} -1)^{-1}$. This allows us to enter the coefficient of increase in the losses in the disks to the losses determined by the average value of the

Due to the gaps between the disks and the protrusion of the field, the magnetic flux density is unevenly distributed, increasing towards the edges of the disk, which leads to an increase in the losses
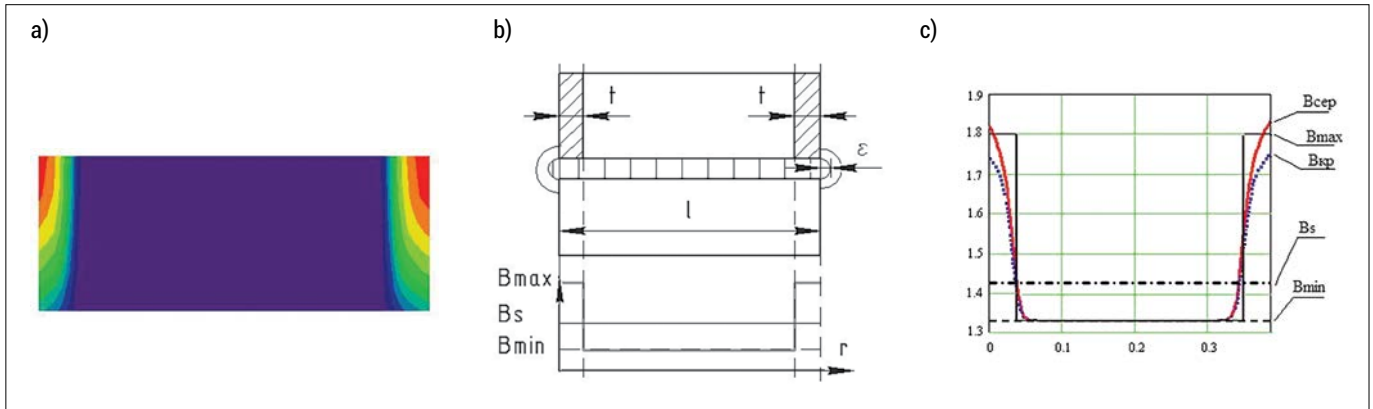
Figure 10. The distribution of magnetic flux density in core stacks: (a) the intensity magnetic flux density in the lower half of the disk, (b) the schematic relation of flux density, (c) the results of a simulation by the MEC of the disk

flux density, according to the expression

$$k_d = (P(B_{min})\cdot(l\text{-}2t)+P(B_{max})\cdot 2t)P(B_s)^{-1}.$$

4.4. Losses due to the non-sinusoidal distribution of the magnetic flux in the yokes

In the yokes of three-phase MSs with side legs, there is a non-sinusoidal flux density distribution due to the branching of the magnetic fluxes of different phases. The maximum value B_m of the flux density and its harmonic components B_i $(i=1,2,3,...)$ determine the coefficient

$$k_u = B_m^{-1}\sqrt{\sum_i\left(i\cdot B_i\right)^2}\,,$$

as well as the empirical dependence

$$\alpha(B_m)=0.177B_m^2-0.33B_m+0.66 \quad [8].$$

The coefficient of loss increase is calculated according to the expression.

$$k_{нc}=\alpha+\left(1-\alpha\right)k_u.$$

4.5. The passage of the magnetic flux in the yokes is not parallel to the rolling of the ES

In the yoke part opposite the main leg, there is an increase in losses due to the passage of the flux, which is not parallel to the rolling direction of the ES.

Thus, for a single-phase reactor of 110 MVAr, Fig. 11(a) shows the distribution of flux density, which is directed across the rolling of steel sheets, and Fig. 11(b) parallel to the sheets. It is known that specific losses increase several times for fluxes in the direction opposite to the steel rolling. The degree of increase depends on the grade of steel, the amplitude

> ## It is known that specific losses increase several times for fluxes in the direction opposite to the steel rolling, and the degree of increase depends on the grade of steel

of the magnetic flux density and the angle between the direction of the flux and the rolling [9]. It is assumed that this increase is 4 units on average, and it is taken into account that the flux density across the roll decreases linearly to zero along the height of the yoke. Therefore, the mass-specific losses in the yokes opposite the main leg are calculated using the formula

$$P_{js} = 4K^{-1}\sum_{i=1}^{K} p\left(B_k i\, K^{-1}\right),$$

where K is the number of flux density calculation points along the height of the yoke, B_k is the flux density in the outer-most disk of the main leg, and $p(B)$ is the specific loss in the ES depending on the flux density according to the corresponding catalogue.

Thus, the coefficient of loss increase is equal to $k_{js}=P_{js}/p(B_k)$. In three-phase reactors, the processes in the zones opposite the main leg are complicated due to the constant change in the flux direction. By comparison with the available test results of a reactor without rod holes in these zones, the coefficient $k_T=2$ was selected to increase the losses P_{js} in three-phase reactors.
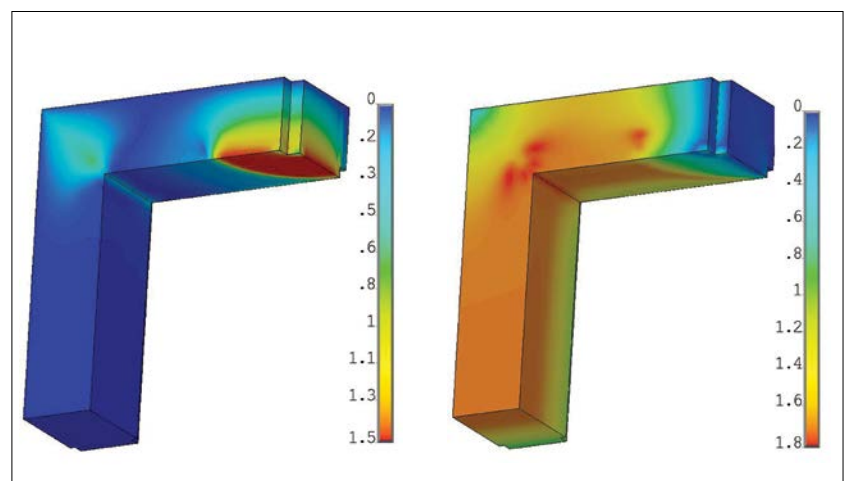
Figure 11. The distribution of magnetic flux density in the yoke and side leg of a single-phase reactor: (a) component directed across the rolling of ES sheets, (b) component parallel to the sheets

In the yokes of three-leg reactors with rod holes, there are fluxes that are directed normally to the ES sheets of the stacks near the rod holes, where eddy currents and corresponding losses are generated

4.6. Losses from eddy currents in the plane of the yoke sheets with holes for the main leg tie rod

In the yokes of three- main leg MSs with rod holes, there are fluxes (4) that are directed normally to the ES sheets of the stacks that are adjacent to the stacks with rod holes, where eddy currents and corresponding losses are generated. For example, Fig. 12 shows the zones of such losses in stacks of the MS yoke with side legs (design (a)) and without side legs (b).

Note that the calculation of losses in ES stacks from the magnetic flux directed normally to the stack plane is performed, in particular, for the end stacks of transformer main legs [6]. As a result of the corresponding calculations, using the specified program, the amount of losses in reactor yoke stacks were obtained depending on the field frequency f, the amplitude of magnetic flux density b, the length L and width H (yoke height) of the sheets, the thickness T of the central stack (with holes): $P_v = k_v \cdot k_p \cdot f^2 \cdot b^2 \cdot (1.2 \cdot L - 200) \cdot H^{2.88} \cdot T$.

The coefficient $k_v = 2.38E\text{-}7$ is obtained for the characteristic dimensions of the yoke. The coefficient $k_p = 0.03$ reflects the character of the field change along the stack thickness, obtained from the results of numerical calculations of losses in the MS yokes of a number of reactors.

4.7. Total losses in magnetic systems of shunt reactors

The main losses are determined by the masses of the corresponding parts of the MC, indicated in Fig. 1b, 1c, and the above loss enhancement factors depicted in Fig. 13.

When the tie rods are placed inside the main legs of three-phase MCs, stray losses due to the eddy currents are added to the main losses.

4.8. The comparison of calculated losses in MS with their estimates during the typical tests of reactors

During the typical electromagnetic tests of ShR, under operating voltage conditions and measured current and ohmic resistance in the winding, the total losses in the reactor and the active losses in the winding and in the taps were measured.

Stray losses in the winding conductors, tank losses, pressing core clamping plates, and tie rods are determined according to calculation methods. For this, the appropriate CAD TER system [5] software was used. Based on the difference between the measured total and all types of specified losses, losses in the MS of the reactor are estimated, which, in principle, corresponds to the standard [1], we denote their value as P_{test}. For example, the table presents the losses according to P_{test} tests and the results of the calculations of P_{calc} losses in MS of single-phase and three-phase reactors according to the methodology presented in this work. In most cases, the error does not exceed 10 %, which can be considered sufficient for the practical design of ShR.
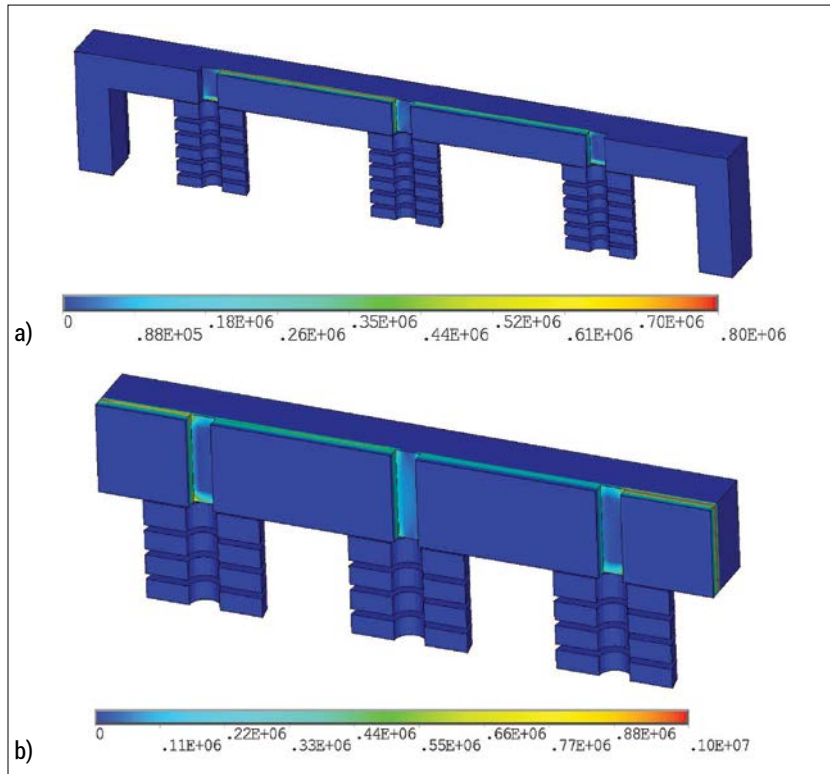
Figure 12. The zones of stray losses due to eddy currents in the MS yoke stacks: (a) design with side legs, (b) without side legs

$$P_o = P_{st} + P_{JT} + P_{JTs} + P_{UG} + P_{JB}, (single\text{-}phase\ MS),$$
$$P_o = P_{st} \cdot 3 + P_{JT} + P_{JF} + P_{JTs} \cdot k_T + P_{JFs}, (three\text{-}phase\ MS\ without\ side\ legs),$$
$$P_o = P_{st} \cdot 3 + P_{JT} + P_{JF} + P_{JTs} \cdot k_T + P_{JFs} + P_{UG} + P_{JB},$$
$(three\text{-}phase\ MS\ with\ side\ legs),$ where
$$P_{st} = k_d \left(p(B_k) \cdot m_{DK} \cdot 2 + p(B_s) \cdot m_{DV} \cdot (n_z - 1) \right), P_{JT} = k_{jt} \cdot p(B_{jt}) \cdot m_{JT} \cdot 4,$$
$$P_{JTs} = \left(k_{jt} \cdot p(B_{jt}) + k_{js} \cdot p(B_k) \right) \cdot m_{JTs} \cdot 4, P_{JF} = k_{jf} \cdot p(B_{jf}) \cdot m_{JF} \cdot 4,$$
$$P_{JFs} = \left(k_{jf} \cdot p(B_{jf}) + k_{js} \cdot p(B_k) \right) \cdot k_T \cdot m_{JFs} \cdot 8,$$
$$P_{UG} = k_{UG}(B_{jt}) \cdot m_{UG} \cdot 4, P_{JB} = k_{jb} \cdot p(B_{jb}) \cdot m_{JB} \cdot 2.$$

Figure 13. Loss enhancement factors

The developed methodology was implemented into the calculation software for the verification calculations of losses in the reactor's MS, as well as in the software for multivariable optimization calculations in the automated system of power transformers and electric reactors design [6].

№	Reactor MVAr/kV/Phase	Ptest, kW	Pcalc, kW	Error, %
1	29.8/36/three	33.4	31.1	-6.9
2	55.0/525/single	19.5	17.9	-8.2
3	110.0/750/single	53.6	42.8	-20.1
4	50.0/500/three	40.8	30.6	-25.0
5	65.0/500/three	38.5	35.3	-8.3
6	70.0/500/three	82.9	81.8	-1.3
7	125.0/500/three	43.1	42.1	-2.3
8	67.0/110/three	45.0	42.2	-6.2
9	120.0/330/three	52.9	49.4	-6.6

5. Conclusion

1. Sequential calculation by interconnected MEC of the main leg with the winding, end, and side legs, as well as the disks of the main leg, ensures the determination of transient magnetic fluxes in the MS of the shunt reactor. The values of these fluxes are necessary and sufficient for the further calculation of losses.

2. In addition to the traditional calculation of the main losses in steel and losses due to the stacking of the sheets, it is necessary to consider the losses due to the non-uniformity of the fluxes in the main leg disks and yoke stacks, non-sinusoidal fluxes, the flux passing across rolled steel, as well as the losses due to eddy currents in the end legs of the MS.

3. The accuracy of loss calculations in the MS of shunt reactors is sufficient for the practice of their design.

Acknowledgments

Bibliography

[1] IEC 60076-6: 2007 *Power transformers - Part 6: Reactors*

[2] M.A. Biki, *Design of electrical reactors for high-voltage power lines on direct and alternating current,* Monolit, Dnepropetrovsk, 164 pages, 2014 (in Russian)

[3] E.A. Mankin, *Calculation of reactors with a steel magnetic core with gaps,* Elektrichestvo, 1959, № 7, pp. 35-41 (in Russian)

[4] L.V. Leltes, *Electromagnetic calculations of transformers and reactors,* Energy, Moscow, 392 pages, 1981 (in Russian)

[5] V.F. Ivankov, *Synthesis and calculation of electric reactors with gaps in the magnetoconductor main leg,* Tekhn. elktrodynamika, 2008, № 3, pp. 66-70 (in Ukrainian)

[6] V.F. Ivankov, A.V. Basova, I.V. Khimyuk, *Methods of modeling transformers and reactors,* Nash format, Kyiv, 490 pages, 2017 (in Ukrainian)

[7] A.N. Kravchenko, V.G. Rodionov, A.I. Shugaylo, I.Ya. Eingorn, *Method for calculating losses and no-load current of transformers,* Tekhn. elektrodinamika, 1979, № 2, pp. 45-52 (in Russian)

[8] Z. Valkovich, P. Veshich, *Calculation of a five-leg core using a digital computer, Rade Končar, Zagreb, pp. 1-24, 1974 (in Russian)*

[9] Z. Cheng, N. Takahashi, B. Forghani, *TEAM Problem 21 Family (V.2009).* (International Compumag Society Board at Compumag, Florianópolis, Brazil, 2009), pp. 1-16, http://www.lmn.pub.ro/~daniel/ElectromagneticModelingDoctoral/Other/ICS-TEAMWorkshop/problem%252021%2520family%2520v%25202009.pdf

[10] Tu P. Minh, Hung B. Duc, Nam P. Hoai, Trinh Tr. Cong, Minh B. Cong, Bao D. Thanh, Vuong D. Quoc, *Finite Element Modeling of Shunt Reactors Used in High Voltage Power Systems, Engineering, Technology & Applied Science Research, Vol. 11, No. 4, 2021, pp. 7411-7416,* https://www.etasr.com/index.php/ETASR/article/download/4271/2549/13488

[11] Özüpak Y., *Designing a Reactor for Use in High Voltage Power Systems and Performing Experimental and Simulation Analysis,* Journal of Engg. Research Online First Article, 2022, pp. 1-14, https://doi.org/10.36909/jer.17017

Authors

Anastasia V. Basova, candidate of technical sciences, leading researcher of the calculation and research laboratory of PrJSC "ZTR", Zaporizhzhia, Ukraine. Her research interests are theoretical electrical engineering, methods of electromagnetic and thermal calculations of structural elements of power transformer equipment based on numerical and analytical models.

Viktor F. Ivankov, candidate of technical sciences, Senior Researcher, ex-head of the calculation and research laboratory of PrJSC "ZTR". His research interests are theoretical electrical engineering, methods of mathematical modeling of electromagnetic, thermal and mechanical processes, computer-aided design systems for power transformers and electrical reactors.